Preprints of the 21st IFAC World Congress (Virtual)
Berlin, Germany, July 12-17, 2020

Time-Optimal Path Following for Robotic Manipulation of Loosely Placed Objects: Modeling and Experiment

Hubert Gattringer * **Andreas Mueller** *
Matthias Oberherber ** **Dominik Kaserer** ***

* *Johannes Kepler University Linz, Institute of Robotics, Austria (e-mail: {hubert.gattringer,a.mueller}@jku.at).*
** *Engel Austria GmbH, Austria (e-mail: matthias.oberherber@engel.at)*
*** *B&R Industrial Automation GmbH, Austria (e-mail: dominik.kaserer@br-automation.com)*

Abstract: A consistent method is presented for solving the so-called general waiter problem, which resembles the general task of manipulating several objects that are loosely placed on a robot, rather than grasped or fixed otherwise. The waiter problem consists of moving a tray (mounted at the end-effector of a robot) with a number of cups, from one pose to another as fast as possible such that the cups do not slide at any time. The geometric path of the tray motion is prescribed while the attitude of the tray must vary. The basis for any optimization and real-time control is a reliable dynamic model of the robot. Therefore a parameter identification is performed using optimized persistent excitation trajectories. The optimization problem is solved with a multiple shooting method which determines the robot trajectory. For the considered wrist-partitioned robot, the motion is described by the joint coordinates of the translation part and the angles describing the orientation of the tray. This combination of joint and task space coordinates is beneficial for solving the optimal control problem (convergence is increased). The optimization accounts for the technical limitations of the robot as well as the limiting friction of the cups. Experimental results with 4 cups for a time-optimal motion are shown. A crucial aspect is the use of a model-based control strategy, along with the identified parameters.

Keywords: Dynamical Modeling, Parameter Identification, Time Optimal Control, Industrial Robotics, Waiter Motion Problem

1. INTRODUCTION

Optimizing robotic systems is mandatory for efficient production in particular in high-wage countries. Time optimal motion is usually restricted by certain technical constraints, like power, motor torques, motor velocities, etc. More sophisticated constraints are gripper forces or constraints due to loosely placed objects on a tray that is mounted at the end-effector (EE) of a robot. This is known as general waiter motion problem introduced in Geu Flores et al. (2011); Geu Flores and Kecskeméthy (2013): only the geometric EE-path is prescribed while the motion along this path as well as the orientation during the motion must be determined. In these publications, a two stage optimization for this problem is presented. First a time optimal initial solution for a fixed spatial EE path is calculated using the so-called Numerical Integration method. In a second optimization stage, intermediate points on the path are introduced and their orientation is varied to decrease the time. Real waiters in catering are very clever in using the orientation of the tray to use centrifugal forces to increase the overall motion speed for delivery. A similar approach discussed in Oberherber et al. (2013) using the so-called Dynamical Programming method to calculate the time optimal solution along a fixed spatial path. A disadvantage of these methods is that the optimized torques exhibit a bang-bang behavior and cannot be applied to a real robot since this can cause damage. In Debrouwere et al. (2013) the whole path including orientation is predefined and additional constraints for preventing objects of tipping over are discussed. An extension to the waiter motion problem is presented in Van Duijkeren et al. (2015). In Luo and Hauser (2015) an iterative learning control method is shown for solving such problems. A slightly different task is discussed in Pham et al. (2013) where the authors present a solution for moving loosely placed objects on a tray below an obstacle. Most publications neglect the effect of viscous joint friction since then the optimization problems become convex leading to better solvability. Further, they do not operate on the allowed limits, i.e. not fully exploit the capabilities of the real physical system or present only simulation results. In contrast to state of the art, in this paper a consistent approach to the waiter motion problem is presented including (i) the identification of the dynamic robot parameters, (ii) a special parametrization of the desired path, (iii) a time-optimal solution using the multiple shooting method, which (iv) can actually be implemented. This approach leads to trajectories that can in fact be implemented and experimentally verified. Instead of a parametric description of the geometric path, a description of the jerk is used, which leads to continuous

motor torques. Experimental results are presented for a Stäubli RX130L industrial robot. The power electronics and industrial PC are replaced by a B&R industrial automation system. This allows for cycle times of 400 μs, to implement model-based control laws, path planning, and to trace all control variables with this cycle time. The robot has 6 degrees of freedom described by joint coordinates $\mathbf{q}^T = (q_1, \ldots, q_6)$. It has a maximum payload of 5 kg and a reachable workspace of approx. 1.5 m. Four cups with liquid are placed at positions $C_1..C_4$ on a tray mounted at the EE of the robot (Fig. 1). The

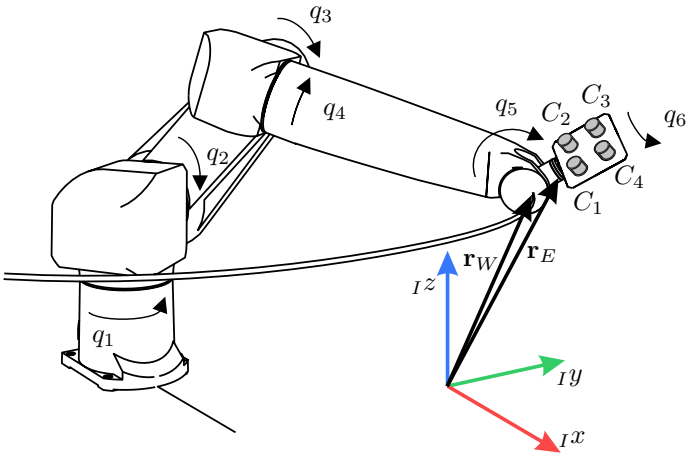

Fig. 1. Waiter motion; Industrial robot and 4 cups.

paper is organized as follows. Section 2 presents the dynamical modeling and parameter identification of the used industrial robot. Path parametrization, the definition of the constraints and the optimization are part of Sect. 3, while Sect. 4 shows the experimental results. In the experiment, 4 cups filled with a liquid are placed loosely on the tray (sloshing is not taken into account).

2. DYNAMIC MODELING AND IDENTIFICATION

2.1 Parameter Identification

Dynamic models are important for trajectory optimization and for model-based control. Therefore an identification of the dynamic parameters of the robot is inevitable. The dynamic motion equations are linear in the dynamic parameters, and can be written as

$$\mathbf{\Theta}_B(\mathbf{q}, \dot{\mathbf{q}}, \ddot{\mathbf{q}})\mathbf{p}_B = \mathbf{Q}_M \tag{1}$$

with the regressor matrix $\mathbf{\Theta}_B$, the base parameters $\mathbf{p}_B$ and the generalized motor torques $\mathbf{Q}_M$, see Neubauer et al. (2014) for details. The linear dependencies in the regressor matrix are already eliminated using a QR decomposition. For the used robot, 40 base parameters have to be identified. Dissipative effects are included as viscous and Coulomb friction. A general procedure is to evaluate (1) with measurements and solve for the unknown base parameters in a least squares sense. However this equation could be badly conditioned since the range of the torques is quite different, e.g the maximum torque for joint 1 is $\mathbf{Q}_{M,1,max} = 1126$ Nm while the torque for the last joint is $\mathbf{Q}_{M,6,max} = 189$ Nm. Therefore a weighting matrix $\mathbf{W}$ is introduced. Then, with (1), the weighted difference of the measured torques and the torques predicted by the model is then

$$\mathbf{e} = \mathbf{W}\left(\mathbf{\Theta}_B\, \mathbf{p}_B - \mathbf{Q}_M\right). \tag{2}$$

The diagonal matrix $\mathbf{W}$ is chosen as

$$\mathbf{W} = \operatorname{diag}\left\{\frac{1}{Q_{M,i,max}}\right\} \tag{3}$$

where $Q_{M,i,max}$ is the maximum torque of the ith robot axis. Doing so, a normalization w.r.t. the maximum torques for every joint is done. For the identification, (2) is evaluated for m measurements, and the resulting overdetermined system of m equations is solved so to minimize the weighted error. The identification accuracy strongly depends on the excitation of the parameters. Therefore a persistent excitation based on Swevers et al. (1997) is implemented. The joint trajectories are chosen as Fourier series

$$q_i(t) = q_{i,0} + \sum_{l=1}^{N_\mathrm{F}} \left(\frac{a_{i,l}}{\omega_0\, l}\, \sin(\omega_0\, l\, t) - \frac{b_{i,l}}{\omega_0\, l}\, \cos(\omega_0\, l\, t) \right), \tag{4}$$

where q_0 is a static position offset, $\mathbf{a}_i, \mathbf{b}_i$ are the Fourier coefficients and ω_0 is the base frequency for the N_F harmonics. A well-conditioned identification problem can be achieved if the condition number of the information matrix $\mathbf{\Theta}_B^T\mathbf{\Theta}_B$ is minimized. This leads to the following optimization problem

$$\min_{\mathbf{q}_0, \mathbf{a}, \mathbf{b}} \operatorname{cond}\left(\mathbf{\Theta}_B^T\mathbf{\Theta}_B\right) \tag{5}$$

$$\text{s.t.} \quad \mathbf{q}_{min} \le \mathbf{q} \le \mathbf{q}_{max} \tag{6}$$

$$|\dot{\mathbf{q}}| \le \dot{\mathbf{q}}_{max} \tag{7}$$

$$|\ddot{\mathbf{q}}| \le \ddot{\mathbf{q}}_{max} \tag{8}$$

$$f\left(\mathbf{q}\right) > 0 \tag{9}$$

with the mechanical joint limits $\mathbf{q}_{min}$ and $\mathbf{q}_{max}$, the maximum joint velocities $\dot{\mathbf{q}}_{max}$ and maximum joint acceleration $\ddot{\mathbf{q}}_{max}$. The indicator function f detects collision of the robot if $f\left(\mathbf{q}\right) \le 0$. The solution of the optimization problem is calculated with an active set solver. In the experiments the parameters $N_F = 5$ and $\omega = 0.8$ rad/s are used. The *Bullet Physics Library* (Coumans (2019)) is used do determine the minimum distance f between the robot and the environment for a collision check during the optimization. A least squares error minimization of (2) leads to the base parameters

$$\mathbf{p}_B = \left(\mathbf{\Theta}_B^T\, \mathbf{W}^T\, \mathbf{W}\, \mathbf{\Theta}_B\right)^{-1}\, \mathbf{\Theta}_B^T\, \mathbf{W}^T\, \mathbf{W}\, \mathbf{Q}_M. \tag{10}$$

Fig. 2 shows a comparison of the measured torques ($Q_{M,i,m}$) and the verification torques ($Q_{M,i,v}$) that are calculated with the identified base parameters $\mathbf{Q}_{M,v} = \mathbf{\Theta}_B\mathbf{p}_B$ (black) for the positioning part of the robot (first three axes). The remaining axes also show excellent matching.

2.2 Control

Execution of time optimal trajectories necessitates application of model-based control schemes since standard linear control methods (PD-joint control) are unable to track the dynamically demanding trajectories. Further, the system is very sensitive to vibrations of the tray since they immediately lead to a loss of contact and sliding of the cups. Therefore, a model-based feed forward in combination with a cascaded PD feedback control are used.

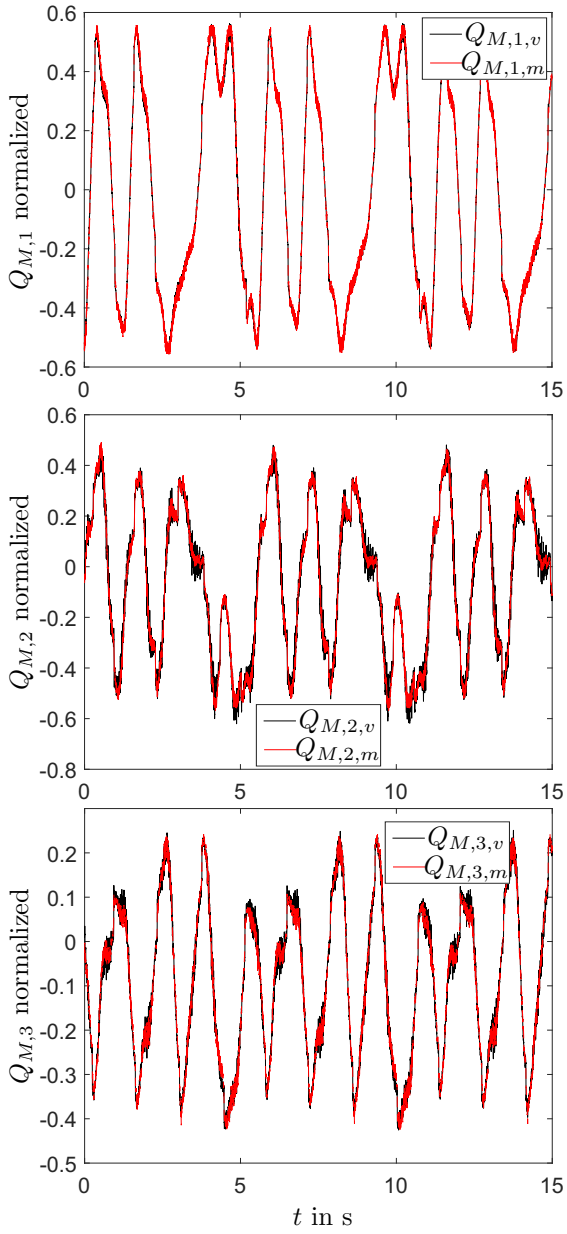

Fig. 2. Verification of identification procedure.

The feed-forward torques $\mathbf{Q}_{M,ff}$ are computed with the identified parameters (sec. 2) as

$$\mathbf{Q}_{M,ff} = \mathbf{\Theta}_B \left(\mathbf{q}_d, \dot{\mathbf{q}}_d, \ddot{\mathbf{q}}_d\right) \mathbf{p}_B. \tag{11}$$

The desired values $\mathbf{q}_d, \dot{\mathbf{q}}_d, \ddot{\mathbf{q}}_d$ are the result from the trajectory optimization.

3. TIME-OPTIMAL TRAJECTORY PLANNING

3.1 Trajectory Description

The task of a waiter is to deliver cups to desired places. It is assumed that the spatial EE path (but not its time evolution) is known while its orientation must be adjusted according to the motion. The used robot is a wrist-partitioned industrial manipulator Siciliano et al. (2009). That is, the joint angles q_1, q_2, q_3 describe the position $\mathbf{r}_W$ of the wrist center, and q_4, q_5, q_6 complete the EE orientation.

The prescribed path of the EE, and thus of the wrist center, is parameterized in terms of a path parameter $s(t)$ as

$$\mathbf{r}_W(t) = \mathbf{r}_W(s(t)). \tag{12}$$

The first three joint angles of the robot are determined by the inverse kinematics, expressed as

$$\left(q_1, q_2, q_3\right)^T = \text{invkin}\left(\mathbf{r}_W\right), \tag{13}$$

which can be computed efficiently Siciliano et al. (2009). The EE motion is thus parameterized by the path parameter and wrist angles summarized in $\mathbf{p} = \left(s, q_4, q_5, q_6\right)^T$.

The prescribed path of the wrist center is defined by B-splines, see Piegl and Tiller (1997)

$$\mathbf{r}_W(s) = \sum_{l=0}^{n_D} N_{l,d}(s)\mathbf{d}_l, \quad s_b \le s \le s_e \tag{14}$$

where $N_{l,d}$ are the B-Spline base functions for $n_D + 1$ control points. A B-Spline of degree $d = 4$ and $n_D = 4$ base function are used. The control points in $\mathbf{d}_l$ determine the shape of the curve. The start and end of the path is normalized to $s_b = 0$ and $s_e = 1$, respectively. Arbitrary spatial paths within the robot workspace are possible. For the test, a path almost resembling a semicircle, which leads to a very dynamic motion is considered. The corresponding control points are listed in Tab. 1. With this parametrization, also velocities and accelerations of $\mathbf{r}_W$ are well defined

$$\dot{\mathbf{r}}_W = \mathbf{r}'_W \dot{s} \tag{15}$$

$$\ddot{\mathbf{r}}_W = \mathbf{r}''_W \dot{s}^2 + \mathbf{r}'_G \ddot{s} \tag{16}$$

where $()' = \partial()/\partial s$ denotes the derivative w.r.t. the path parameter s.

Table 1. Control points

	CP_1	CP_2	CP_3	CP_4	CP_5
x in m	0.01	1.3	1.8	1.3	0.01
y in m	1.2	1.2	0	-1.2	-1.2
z in m	0.2	0.2	0.2	0.2	0.2

3.2 Non-Slipping Condition

To ensure that objects loosely placed on a tray do not slide, a sticking condition has to be fulfilled

$$\mathbf{f}_T \le \mu_0 \mathbf{f}_N \tag{17}$$

where $\mathbf{f}_T$ and $\mathbf{f}_N$ are tangential and normal forces of the object. The static friction coefficient μ_0 can be identified via $\tan \rho = \mu_0$ with the angle ρ where sliding starts. Figure 3 shows the friction cone of one of the cups on the tray at the EE. Using Newton's law of motion $\mathbf{f} = m\mathbf{a}$, the non-slipping condition of the ith object (cup) can be written as

$$\sqrt{{}_E a_{x,i}^2 + {}_E a_{y,i}^2} \le \mu_0 \; {}_E a_{z,i}. \tag{18}$$

Here, ${}_E\mathbf{a}_i = \left({}_E a_{x,i}, {}_E a_{y,i}, {}_E a_{z,i}\right)^T$ is the acceleration of the ith object represented in EE frame of the robot. They are determined by

$${}_E\mathbf{a}_i = \mathbf{R}_{EI}({}_I\ddot{\mathbf{r}}_W + {}_I\ddot{\mathbf{r}}_{WE} + {}_I\ddot{\mathbf{r}}_{Ei} - {}_I\mathbf{g}) \tag{19}$$

where $\mathbf{g}$ is the gravity vector, $\mathbf{r}_{WE}$ is the vector from the wrist center to the EE, and $\mathbf{r}_{Ei}$ is the vector from the EE to the position of the ith object on the tray, see again Fig. 3. The rotation matrix $\mathbf{R}_{EI}$ transforms vectors from inertial to EE frame. The cup positions are listed in Tab. 2

3.3 Optimal Control Problem

With the path planning and non-slipping constraints, time/energy optimal trajectories for the Waiter Motion Problem can be computed. As mentioned in Sect. 3.1 well suited optimization variables are $\mathbf{p}^T = (s \;\; q_4 \;\; q_5 \;\; q_6)$. There are several methods to obtain smooth trajectories, e.g. B-Spline parametrization. Here the jerk of the optimization variables is used as input

$$\mathbf{u} = (\dddot{s}, \dddot{q}_4, \dddot{q}_5, \dddot{q}_6)^T \tag{20}$$

in order to obtain a smooth trajectory. By introducing a state vector

$$\mathbf{x}^T = \left(\mathbf{p}^T, \dot{\mathbf{p}}^T, \ddot{\mathbf{p}}^T\right) \tag{21}$$

the connection between optimization variables and input variables is given by an integrator chain

$$\dot{\mathbf{x}} = \begin{bmatrix} 0 & \mathbf{I} & 0 \\ 0 & 0 & \mathbf{I} \\ 0 & 0 & 0 \end{bmatrix} \mathbf{x} + \begin{pmatrix} 0 \\ 0 \\ \mathbf{I} \end{pmatrix} \mathbf{u} := \mathbf{f}(\mathbf{x}, \mathbf{u}) \tag{22}$$

which is included as equality constraint in the optimization problem (identity matrix $\mathbf{I}$). The overall optimization problem can be formulated as

$$\min_{t_e, \mathbf{u}} \quad \int_0^{t_e} 1 + k\mathbf{u}^T\mathbf{u} \; dt \tag{23}$$

subject to

$$|\dot{\mathbf{q}}| \leq \dot{\mathbf{q}}_{max} \tag{24}$$

$$|\mathbf{\Theta}_B(\mathbf{q}, \dot{\mathbf{q}}, \ddot{\mathbf{q}})\mathbf{p}_B| \leq \mathbf{Q}_{M,max} \tag{25}$$

$$\sqrt{{}_E a_{x,i}^2 + {}_E a_{y,i}^2} \leq \mu_0 \; {}_E a_{z,i}, \quad i = 1, \ldots, N_{\text{Cups}} \tag{26}$$

$$\dot{\mathbf{x}} = \mathbf{f}(\mathbf{x}, \mathbf{u}) \tag{27}$$

$$\mathbf{q}(0) = \mathbf{q}_0, \quad \dot{\mathbf{q}}(0) = 0, \quad \ddot{\mathbf{q}}(0) = 0 \tag{28}$$

$$\mathbf{q}(t_e) = \mathbf{q}_e, \quad \dot{\mathbf{q}}(t_e) = 0, \quad \ddot{\mathbf{q}}(t_e) = 0 \tag{29}$$

$$\mathbf{u} \leq \mathbf{u}_{max} \tag{30}$$

$$0 \leq s \leq 1 \tag{31}$$

$$\dot{s} \geq 0 \tag{32}$$

$$s(0) = 0, s(t_e) = 1. \tag{33}$$

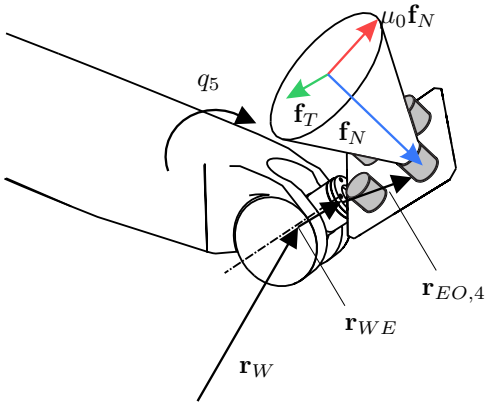

Fig. 3. Friction cone of a cup on the tray.

Table 2. Position of cup $i = 1, \ldots, 4$

	Cup 1	Cup 2	Cup 3	Cup 4
${}_E r_{Ei,x}$ in m	0.14	0.14	0.24	0.24
${}_E r_{Ei,y}$ in m	-0.065	0.065	0.055	-0.055
${}_E r_{Ei,z}$ in m	0.02	0.02	0.02	0.02

The cost functional in (23) is a trade-off between minimal time t_e and minimal overall jerk, determined by the weight k. Inequality constraints (24,25) account for the maximum joint velocities $\dot{\mathbf{q}}_{max}$, motor torques $\mathbf{Q}_{M,max}$, the non-slipping condition (26), and jerk limits (input of the integrator chain) (30). The dynamical system (27) represents the integrator chain. Equality constraints (29) account for the initial (28) and terminal values of the joint positions, velocities, and accelerations, as well as of the path parameter (33). Note, q_1, q_2, q_3 and derivatives are calculated from $\mathbf{r}_W(s)$ within the optimization. We use MUSCOD II optimization software (Kuhl et al. (2001)) developed at the University of Heidelberg. The software uses a direct multiple shooting method, see Leineweber (1999) for details. In order to account for model uncertainties, the maximum values used within the optimization are set 90% of technical/physical limits. The maximum motor velocities and torques are listed in Tab. 3, where $J_i, i = 1, \ldots, 6$ stands for the ith joint. The maximal acceleration and jerk for the wrist joints are set to $\ddot{q}_{i,max} = 200$ rad/s^2, $\dddot{q}_{i,max} = 1000$ rad/s^3, $i = 4, 5, 6$, and for the path parameter $s\,(t)$ the limits $\ddot{s}_{max} = 200$ 1/s^2, $\dddot{s}_{max} = 1000$ 1/s^3 are used. The static friction coefficient was identified as $\mu = 0.34$ using simple sliding experiments.

Table 3. Maximal torque and velocity of joint J_i.

	J_1	J_2	J_3	J_4	J_5	J_6
$\mathbf{Q}_{M,max}$ in Nm	1126	1126	849	264	615	189
$\dot{\mathbf{q}}_{max}$ in rad/s	4.3	4.3	5.5	6.4	7.5	17.6

3.4 Optimization Results

The optimal control problem was numerically solved with the multiple shooting method. In order to achieve convergence, a discretization into $n = 250$ shooting intervals was necessary. The (nearly) time optimal solution results in $t_e = 1.35$ s, where in (23) the weight $k = 10^{-5}$ was used.

Figure 4 shows the optimized joint velocities $\dot{\mathbf{q}}$ and the path velocity $\dot{s}$ normalized to their respective maximum value. In Fig. 5 the optimized motor torques are depicted. It can be seen that the velocity $\dot{q}_1$ and the torque Q_{M1} are temporarily at their limit, indicating time-optimal motion.

The tangential accelerations ${}_E a_{T,i} := \sqrt{{}_E a_{x,i}^2 + {}_E a_{y,i}^2}$ of the four cups, which is limited by (26) in order prevent

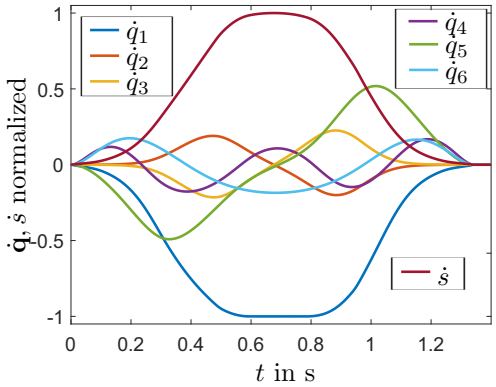

Fig. 4. Optimized Velocities.

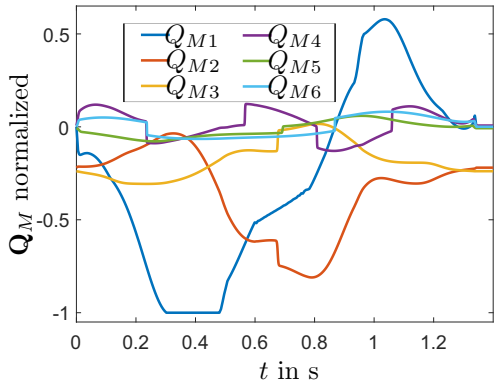

Fig. 5. Optimized Torques.

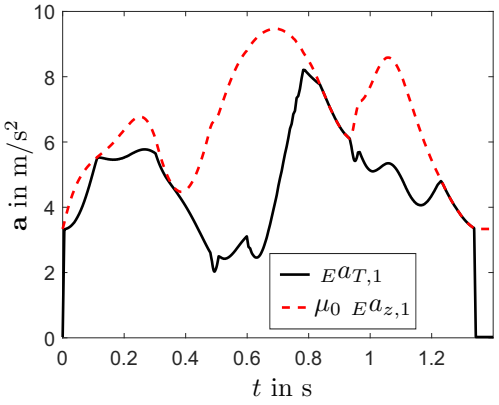

Fig. 6. Acceleration constraint for the cup 1.

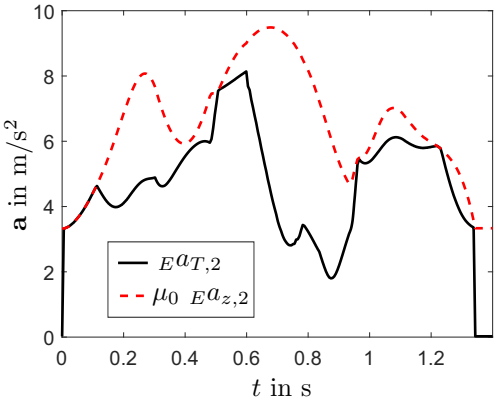

Fig. 7. Acceleration constraint for the cup 2.

slipping, are shown Fig. 6-9. Apparently, one of the tangential forces, torques or velocities is always at its allowed limit, which again indicates a time-optimal solution. In summary, during most part of motion either the tangential force of one of the cups, the joint velocities, or the motor torques are at their allowed limits. The non-slipping constraints (26) are mainly active at the begin and at the end of the trajectory. Another interesting optimization result is the behavior of the wrist axes, which are mainly responsible for the orientation of the EE, see Fig. 10 and 3. Especially angle q_5 determines the tilting of the tray about the instantaneous tangent to the motion curve. A large angle of approx. 75° is necessary due to the fast motion and the corresponding centrifugal forces. A photograph of an extreme position in the middle of the trajectory is depicted in Fig. 11.

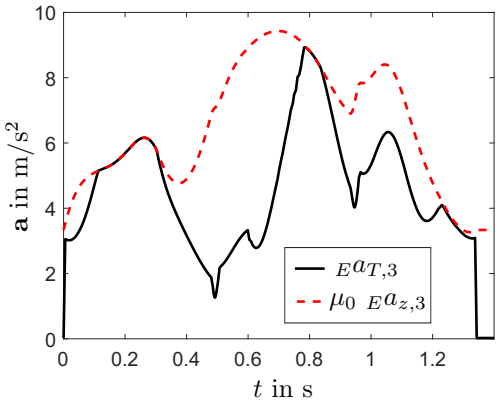

Fig. 8. Acceleration constraint for the cup 3.

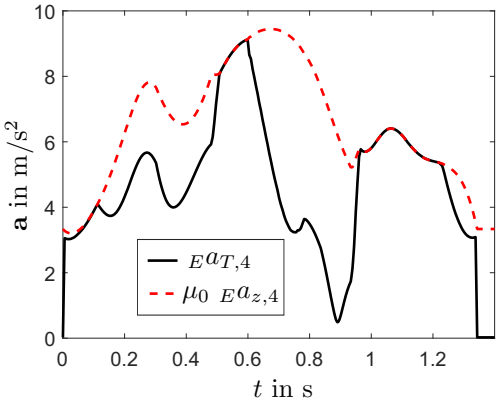

Fig. 9. Acceleration constraint for the cup 4.

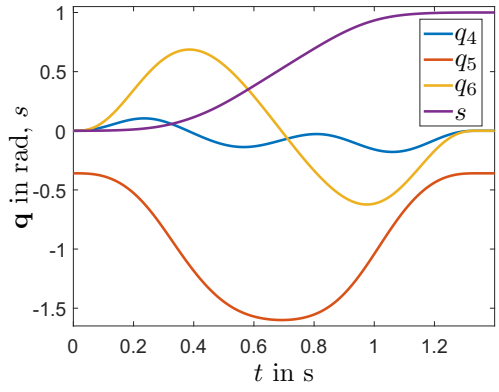

Fig. 10. Optimal solution for s, q_4, q_5, q_6.

The maximal velocity and acceleration of the cups is $v_{E,max} = 6.2$ m/s and $a_{E,max} = 27$ m/s^2, respectively. A video of this really high dynamic motion can be found at *https://www.youtube.com/watch?v=O2Aptb5VqMg* .

Fig. 11. Extreme cup position

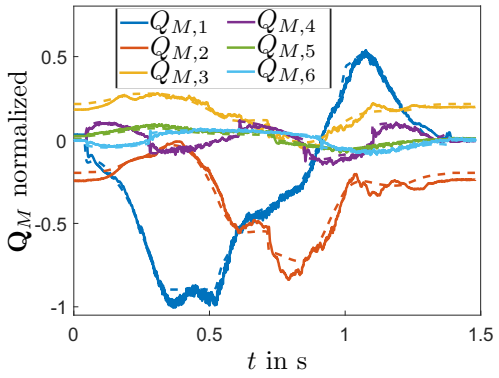

Fig. 12. Motor torques normalized to maximum value.

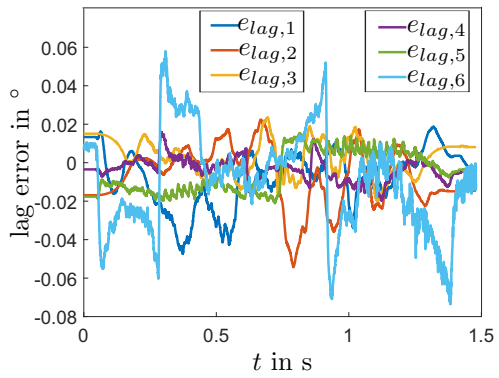

Fig. 13. Joint tracking errors.

4. EXPERIMENTAL RESULTS

Figure 12 shows the feedforward torques $\mathbf{Q}_{M,ff}$ computed from the model (dashed lines) and the measured torques (solid lines) when executing the optimized trajectory. The experimental and theoretical values match well. There are slight differences when high torques are required. One reason could be that during the identification procedure in Sect. 2 the torques are not at their limit. Further, viscous and Coulomb friction was assumed, and also nonlinear behavior is known to appear for higher velocities. Another simplification is that the motor torque is assumed linearly related to the motor current as $M_{Mot} = k_m I_{Mot}$. Also the nonlinear characteristics of the power electronics is neglected, which is significant especially for high torques. The tracking errors $\mathbf{e}_{lag} = \mathbf{q}_d - \mathbf{q}$ of the joint angles are shown in Fig. 13. They are very low leading to a successful experiment. Results for the accelerations are not directly accessible since no acceleration sensor at the EE is available. They can be calculated by differentiating the measured joint positions and applying forward kinematics.

5. CONCLUSION

Mathematical model and the control problem are derived for the generalized waiter motion with 4 cups, which is an example for the general optimal control problem of manipulating loosely placed objects. A parameterization in terms of the path parameter and the wrist angles is introduced, which aids the numerical solution of this control problem using a multiple shooting method. Experimental results are shown that very well match the theoretically expected behavior. Crucial for actually executing the time-optimal trajectories is the application of a model-based feedforward control. Future work will extend the model to take into account the fluid in the cups and to prevent sloshing. Additional constraints for avoiding tip over of the objects will also be included.

ACKNOWLEDGEMENTS

This work has been supported by the "LCM – K2 Center for Symbiotic Mechatronics" within the framework of the Austrian COMET-K2 program.

REFERENCES

Coumans, E. (2019). *Bullet Physics Library.* `www.bulletphysics.org`.

Debrouwere, F., Loock, W., Pipeleers, G., Diehl, M., Swevers, J., and Schutter, J. (2013). Convex time-optimal robot path following with cartesian acceleration and inertial force and torque constraints. *Journal of Systems and Control Engineering*, 227, 724–732.

Geu Flores, F. and Kecskeméthy, A. (2013). Time-optimal path planning for the general waiter motion problem. In *Advances in Mechanisms, Robotics and Design Education and Research*, 189–203. Springer Verlag.

Geu Flores, F., Kecskeméthy, A., and Pöttker, A. (2011). Time-optimal motion planning along specified paths for multibody systems including dry friction and power constraints. In *13th World Congress in Mechanism and Machine Science*.

Kuhl, P., Ferreau, J., Albersmeyer, J., Kirches, C., Wirsching, L., Sager, S., Potschka, A., Schulz, G., Diehl, M., Leineweber, D., and Schafer, A. (2001). Muscod-ii users' manual.

Leineweber, D. (1999). Efficient reduced sqp methods for the optimization of chemical processes described by large sparse dae models. *Fortschritt-Berichte VDI Reihe 3*, 613.

Luo, J. and Hauser, K. (2015). Robust trajectory optimization under frictional contact with iterative learning. In *Robotics, Science and Systems (RSS)*.

Neubauer, M., Gattringer, H., and Bremer, H. (2014). A persistent method for parameter identification of a seven-axes manipulator. *Robotica*, 33, 1099–1112.

Oberherber, M., Gattringer, H., and Springer, K. (2013). A time optimal solution for the waiter motion problem with an industrial robot. In *Proceedings of the Austrian Robotics Workshop (ARW) 2013*, 55–60.

Pham, Q.C., Caron, S., and Nakamura, Y. (2013). Kinodynamic planning in the configuration space via admissible velocity propagation. In *Proceedings of Robotics: Science and Systems*.

Piegl, L.A. and Tiller, W. (1997). *The NURBS book*. Springer Verlag.

Siciliano, B., Sciavicco, L., Villani, L., and Oriolo, G. (2009). *Robotics - Modelling, Planning and Control*. Springer Verlag.

Swevers, J., Ganseman, C., Tükel, D., Schutter, J.D., and Brussel, H.V. (1997). Optimal robot excitation and identification. *IEEE Transactions on Robotics and Automation*, 13, 730–740.

Van Duijkeren, N., Debrouwere, F., Pipeleers, G., and Swevers, J. (2015). Cartesian constrained time-optimal point-to-point motion planning for robots: The waiter problem. In *Benelux Meeting on Systems and Control. Belgium*.